Nonisothermal Models for Soil–Water Retention Curve

Farshid Vahedifard, M.ASCE[1]; Toan Duc Cao, A.M.ASCE[2]; Sannith Kumar Thota, S.M.ASCE[3]; and Ehsan Ghazanfari, M.ASCE[4]

Abstract: Several emerging problems in geotechnical and geoenvironmental engineering pose multiphysics problems involving nonisothermal processes in unsaturated soils. Properly studying these problems requires the development of models for the soil water retention curve (SWRC) to describe the constitutive behavior of unsaturated soils under nonisothermal conditions. This study aims to develop analytical expressions of nonisothermal SWRCs. Closed-from expressions are presented to consider the effects of temperature on adsorption and matric suction in unsaturated soils. The formulation for the nonisothermal matric suction accounts for the effects of temperature on the surface tension, soil–water contact angle, and adsorption by the enthalpy of immersion per unit area. The formulations are then used to extend several existing isothermal SWRCs to nonisothermal conditions. The extended SWRC models are used in a parametric study to examine changes in adsorbed water, capillary water, and total water content versus matric suction for Ottawa sand and Wyoming bentonite subjected to several temperatures ranging from 25 to 100°C. The results show that temperature can have significant effects on SWRCs, depending upon the soil type and range of temperature. Further, the results obtained from the proposed formulations are compared against three independent laboratory test results and very good agreement is observed with the tests conducted on sand, silt, and clay under different temperatures. The proposed formulations can be readily incorporated into analytical solutions and numerical simulations of thermo-hydro-mechanical models of unsaturated soils. The findings of the study can facilitate using numerical models to simulate various nonisothermal applications involving geo-energy systems and soil-atmospheric interaction problems. **DOI: 10.1061/(ASCE)GT.1943-5606.0001939.**

Author keywords: Unsaturated soil; Soil water retention curve; Nonisothermal; Suction; Temperature; Capillary water; Adsorption.

Introduction and Background

The soil water retention curve (SWRC) is a key constitutive relationship to describe the behavior of unsaturated soils. The SWRC establishes a relationship between a measure of water content (commonly represented by volumetric water content or saturation) and matric suction (i.e., the difference between the pore air pressure and pore water pressure). SWRC can be directly measured in the laboratory or field. Further, there are several parameterized models in the literature to represent SWRC (e.g., Brooks and Corey 1964; van Genuchten 1980; Fredlund and Xing 1994). These models establish the relationship between water content and suction using a functional form including a number of fitting parameters. The level of complexity and the number of fitting parameters are different among these models. The majority of the existing SWRC models are developed for isothermal conditions (i.e., no change in temperature or no effect due to temperature change). However, there are several emerging problems including climate change, disposal and storage of nuclear waste, radioactive barriers, buried high voltage cables, ground-source heat pumps for geothermal heating/cooling systems, soil-borehole thermal energy storage systems, and thermally active earthen structures, which all require considering nonisothermal conditions in unsaturated soils (e.g., Coccia and McCartney 2012; McCartney et al. 2013; Vahedifard et al. 2015, 2016, 2017; Alsherif and McCartney 2015; Robinson and Vahedifard 2016). Soil temperature in some of these applications (e.g., disposal and storage of nuclear waste) may reach to a thermal limit of 100°C (Hicks et al. 2009). Further, several studies have been conducted to evaluate chemical, mechanical, and geological alterations in bentonite and clay-rock formations as a result of hydration and/or heating at high temperatures up to 300°C (e.g., Zheng et al. 2015; Ma and Hueckel 1992; Wersin et al. 2007).

Previous studies have shown that the SWRC is affected by several factors including, but not limited to, pore size distribution, chemical composition, temperature, and adsorption capacity (e.g., Grant and Salehzadeh 1996; Villar and Lloret 2004; Lu 2016). Several researchers have studied the effects of temperature on the SWRC over the past few decades. Previous studies include performing experimental tests to examine changes in the SWRC caused by varying temperature, and extending the existing SWRC models by including temperature-dependent terms to account for nonisothermal conditions (e.g., Grant and Salehzadeh 1996; Schneider and Goss 2011; Bachmann et al. 2002; Wan et al. 2015; Romero et al. 2001; Salager et al. 2007; Villar and Lloret 2004; Tang and Cui 2005; Vilar and Gomez-Espina 2007; Uchaipichat and Khalili 2009; Jacinto et al. 2009; Salager et al. 2010; Zhou et al. 2014; Roshani and Sedano 2016). Experimental results have generally shown that an elevated temperature causes a downward shift in the SWRC shape, leading to a decrease in saturation

[1]Associate Professor, Dept. of Civil and Environmental Engineering, Mississippi State Univ., Mississippi State, MS 39762 (corresponding author). Email: farshid@cee.msstate.edu

[2]Postdoctoral Associate, Dept. of Civil and Environmental Engineering, Center for Advanced Vehicular Systems, Mississippi State Univ., Mississippi State, MS 39762. Email: toand@cavs.msstate.edu

[3]Graduate Student, Dept. of Civil and Environmental Engineering, Mississippi State Univ., Mississippi State, MS 39762. Email: st1545@msstate.edu

[4]Assistant Professor, Dept. of Civil and Environmental Engineering, Univ. of Vermont, Burlington, VT 05405. Email: Ehsan.Ghazanfari@uvm.edu

Note. This manuscript was submitted on June 16, 2017; approved on March 29, 2018; published online on July 2, 2018. Discussion period open until December 2, 2018; separate discussions must be submitted for individual papers. This paper is part of the ***Journal of Geotechnical and Geoenvironmental Engineering***, © ASCE, ISSN 1090-0241.

(or volumetric water content) under a constant suction (e.g., Grant and Salehzadeh 1996). The temperature-dependency of the SWRC is attributed to temperature-induced changes in the surface tension of the pore water, soil–water contact angle, soil fabric, water absorption potential, and pore size distribution (e.g., Grant and Salehzadeh 1996; Romero et al. 2001). However, the extent of temperature effects varies based upon various parameters including soil type, soil mineralogy, range of temperature, range of suction, saturation levels, soil confinement, among others (e.g., Romero et al. 2001; Villar and Lloret 2004; Romero et al. 2003; François and Ettahiri 2012; Wan et al. 2015).

Mechanisms by which temperature affects the water retention capacity of a soil vary depending upon the soil's water content. For high water contents, the interaggregate porosity containing the bulk water or free water presents the capillary storage mechanism. In this region, capillary effects dominate the water retention capacity and elevated temperatures can lead to reduced surface tension, expansion of trapped air bubbles, isolated water packets, and changes in the quantity of solute (Schneider and Goss 2011; Romero et al. 2001, 2003). For low water contents, however, several of the aforementioned effects of temperature are no longer applicable. This is because the pores are no longer filled with water in dry conditions and the binding of the water is not dominated by capillary forces but rather by adsorptive forces. In this region, intra-aggregate porosity controls the retention capacity through the adsorption storage mechanism and contains quasi-immobile water. For clays with low water contents, the main temperature effects on the water retention capacity are due to thermo-chemical changes affecting clay fabric and quasi-immobile water as well as the chemically-induced water adsorption potential (Romero et al. 2001; Villar and Lloret 2004; Villar et al. 2005).

Although a number of attempts have been made to incorporate the effects of temperature into SWRC models, several gaps remain to be filled. The majority of existing nonisothermal SWRC models only consider the interfacial surface tension as the sole temperature-dependent variable and ignore the effects of temperature on other parameters (e.g., Philip and de Vries 1957; Salager et al. 2007; Zhou et al. 2014; Wan et al. 2015; Roshani and Sedano 2016). Experimental tests, however, show that considering the surface tension as the only temperature-dependent component is not sufficient to explain the effects of temperature on the SWRC (Bachmann et al. 2002). Temperature effects on other parameters such as the contact angle and adsorption (e.g., Bachmann et al. 2002; Schneider and Goss 2011; Grant and Salehzadeh 1996) have been studied. However, there is still a need for developing nonisothermal SWRC models, which properly account for the effects of temperature on most, if not all, of influential factors.

This study presents analytical expressions to consider the effects of temperature on two main storage mechanisms (i.e., adsorption and capillarity) in unsaturated soils. The formulation for the matric suction, representing capillary pressure in unsaturated soils, accounts for the effects of temperature on surface tension, contact angle, and adsorption by the enthalpy of immersion per unit area. The formulations are then used to extend several existing isothermal SWRCs to nonisothermal conditions. The extended SWRC models are used in a parametric study to examine changes in adsorbed water, capillary water, and total water content versus matric suction for Ottawa sand and Wyoming bentonite subjected to several temperatures ranging from 25 to 100°C. Further, the results from the proposed formulations are compared against independent experimental test results reported in the literature.

Water Retention Mechanisms: Adsorbed and Capillary Water

Incorporating the impacts of temperature into SWRC models warrants studying the effects of temperature on different water retention mechanisms in soil. The total retained water in soil can be defined as the summation of adsorbed and capillary waters (e.g., Romero et al. 2001; Revil and Lu 2013; Lu 2016):

$$\theta = \theta_a + \theta_c \tag{1}$$

where θ = total water content retained in soil; θ_a = adsorbed water; and θ_c = capillary water. The adsorbed water can be in the form of hygroscopic or hydration water forming a bounded thin liquid film of water around the surface of the particles. The capillary water is free or bulk water retained in pore corners behind curved interfaces (Revil and Lu 2013; Lu 2016).

The total amount of adsorbed water is typically small compared with the volumetric contribution of capillary water, and its contribution is important for processes such as microbial activity, plant water uptake, and evaporation in dry environments (e.g., Lu 2016). Adsorption of water on soil particles is the dominant water storage mechanism at high suctions (McQueen and Miller 1974) and is mainly due to van der Waals forces that enable the formation of liquid films around soil particles (Mitchell and Soga 2005). Adsorbed water is strictly linked to the soil specific surface area and is important in determining processes related to contaminant adsorption, ion exchange reactions, microbial attachment to solid particles, and heat transfer. Khorshidi et al. (2016) identified three types of adsorption that occur in clay and silt, each with different physical origins and operating ranges: cation hydration, inner surface hydration, and particle surface hydration. In the cation hydration range, the water is strongly bonded to the exchangeable cations and the water retention regime is considered tightly adsorbed (Khorshidi et al. 2016). Several models have been proposed for the SWRC and hydraulic conductivity function that take into account the adsorption under isothermal conditions (e.g., Tuller and Or 2005b; LeBeau and Konrad 2010; Revil and Lu 2013).

Tuller et al. (1999) used a modified form of the Young–Laplace equation that considers capillary and adsorptive contributions to the matric potential to calculate liquid–vapor interfaces within a cross section of their angular pore model. When studying the capillary contribution, it is important to consider the adsorption by surface enthalpy, which is referred to as the enthalpy required to create a unit area of surface. Tuller et al. (1999) used a unit cell concept, shown in Fig. 1, to illustrate the liquid–vapor interface transitioning from adsorption to capillary-dominated imbibition. Tuller et al. (1999) used the unit cell concept to propose a new model for pore space geometry, with an attempt to properly capture both adsorption processes in an internal surface area and capillary behavior in

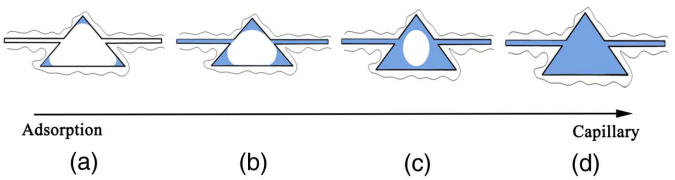

Fig. 1. Conceptual sketch of liquid–vapor interface transitioning from adsorption to capillary-dominated imbibition: (a) low matric potentials where liquid films adsorbed on pore and slit walls and liquid held in corners due to capillary forces; (b) capillary condensation; (c) pore snap off; and (d) complete saturation. (Modified from Tuller and Or 2005a.)

angular pore spaces. The potential of accommodating adsorptive surface forces leads to a more accurate derivation of the SWRC for porous media with high specific surface areas (i.e., clay) under dry conditions. In the following sections, closed-form expressions are presented to account for the effects of temperature on various components contributing to the adsorbed and capillary water.

Temperature Effects on Soil Water Retention Curve

Temperature Effects on Adsorbed Water

The Freundlich model (Ponec et al. 1974; Jeppu and Clement 2012) can be used to describe the amount of adsorbate (liquid) on a flat adsorbent (solid) in thermodynamic energy equilibrium with the ambient adsorbate (in vapor phase) as follows:

$$\theta_a = \theta_a^{\max}(RH)^{1/M} \tag{2}$$

where $\theta_a^{\max}$ = adsorption capacity; RH = relative humidity; and M = adsorption strength, a fitting parameter primarily controlled by mineral type and quantity. By imposing a form of the Kelvin–Laplace equation, Revil and Lu (2013) rewrote Eq. (2) as follows:

$$\theta_a = \theta_a^{\max}\left[\exp\left(-\frac{M_w\psi}{RT}\right)\right]^{1/M} \tag{3}$$

where $M_w = 1.8 \times 10^{-5}$ m^3 mol^{-1} and is the molar volume of water; $R = 8.314$ J mol^{-1} K^{-1} = universal gas constant; ψ = matric suction in Pa, representing capillary pressure in unsaturated soils; and T = temperature in Kelvin.

Several studies have found that the adsorbed water may degenerate to capillary water at very high temperatures (e.g., Powers 1967; Derjaguin et al. 1986; Ma and Hueckel 1992). Derjaguin et al. (1986) reported that this phenomenon can start happening at a temperature of about 70°C.

Temperature Effects on Capillary Water

Matric suction can be described using the Young–Laplace equation (Young 1805; Lu and Likos 2004):

$$\psi = u_a - u_w = \frac{2\sigma\cos\alpha}{r} \tag{4}$$

where u_a = pore–air pressure (conventionally referenced as zero for surface and near surface applications by measuring all pressure terms relative to the atmospheric pressure); α = soil–water contact angle of the fluid–fluid interface with the solid; u_w = pore–water pressure; r = pore size (the average radius of the water-air interface); and σ = water–air surface tension. The partial derivative of ψ with respect to temperature can be written as (Bachmann et al. 2002):

$$\frac{\partial\psi}{\partial T} = \frac{\psi}{\sigma}\frac{\partial\sigma}{\partial T} + \frac{\psi}{\cos\alpha}\frac{\partial(\cos\alpha)}{\partial T} \tag{5}$$

Philip and de Vries (1957), and several others (e.g., Imbert et al. 2005; Salager et al. 2007; Uchaipichat and Khalili 2009; Zhou et al. 2014; Wan et al. 2015; Roshani and Sedano 2016), ignored the second term in the right-hand side of Eq. (5) assuming that α is independent of temperature, although a study by Bachmann et al. (2002) demonstrated that the contact angle does depend on temperature. In the current study, we incorporate the effect of temperature on the contact angle, as explained in the following section.

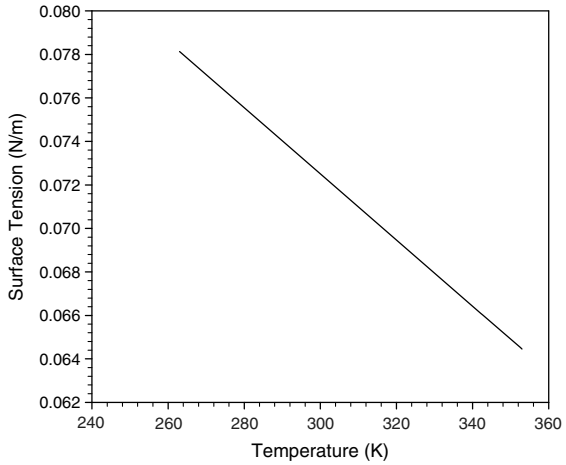

Fig. 2. Variation of surface tension with temperature for pure water.

Water–Air Surface Tension

The effect of temperature on the water–air surface tension can be described using a linear function as (Haar et al. 1984; Dorsey 1940)

$$\sigma = a' + bT \tag{6}$$

where a' and b = fitting parameters. Using regression analysis through the reference interfacial tension data, Haar et al. (1984) and Dorsey (1940) proposed the following estimations for a' and b coefficients

$$\begin{aligned} a' &= 0.11766 \pm 0.00045 \text{ Nm}^{-1} \\ b &= -0.0001535 \pm 0.0000015 \text{ Nm}^{-1}\text{ K}^{-1} \end{aligned} \tag{7}$$

Fig. 2 shows the variation of surface tension with temperature for pure water using Eq. (6) in the range of temperature from 263 to 353 K.

Soil–Water Contact Angle

Grant and Salehzadeh (1996) showed that by considering a temperature-dependent contact angle, the temperature derivative of the wetting coefficient, $\cos\alpha$, can be expressed in terms of independently measurable physical–chemical quantities as follows:

$$\frac{d\cos\alpha}{dT} = \frac{1}{\sigma}\left(\frac{\sigma\cos\alpha + \Delta h}{T} - \cos\alpha\frac{d\sigma}{dT}\right) \tag{8}$$

where Δh = enthalpy of immersion per unit area. The enthalpy can be determined by experimental measurements or by using the differential enthalpy of adsorption of the vapor (Everett 1972). In the current study, the following equation is used to model the enthalpy reduction by increasing the temperature (Watson 1943):

$$\Delta h = \Delta h_{(T_r)}\left(\frac{1 - T_r}{1 - T}\right)^{0.38} \tag{9}$$

where $\Delta h_{(T_r)}$ = enthalpy of immersion per unit area at a reference temperature T_r. Per Harkins and Jura (1944), Δh_{T_r} can be determined using the water–air surface tension and the wetting coefficient at T_r. The solution of Eq. (8) allows the calculation of the wetting coefficient, $\cos\alpha$, as a function of temperature. By substituting Eq. (6) into Eq. (8), a general form can be obtained as follows:

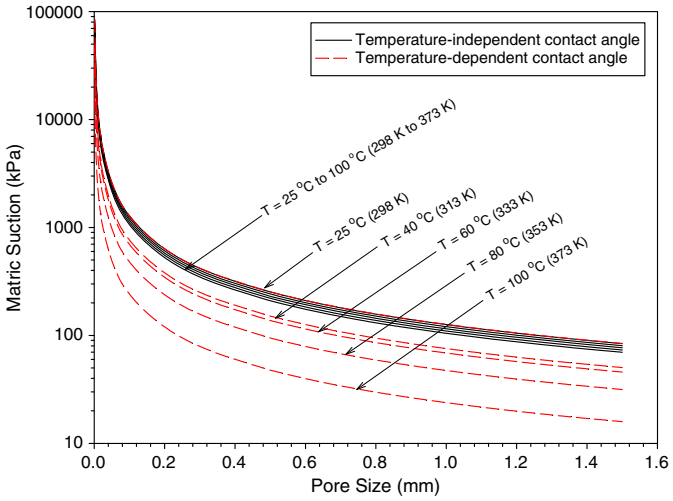

Fig. 3. Relationship between matric suction and pore size for temperature-independent and temperature-dependent contact angles at various temperatures.

$$(a'T + bT^2)\frac{d\cos\alpha}{dT} - a'\cos\alpha = \Delta h \tag{10}$$

Solving Eq. (10) for $\cos\alpha$ yields the temperature-dependent form of the contact angle as follows:

$$\cos\alpha = \frac{-\Delta h + TC_1}{a' + bT} \tag{11}$$

where C_1 = constant, which can be determined as (Grant and Salehzadeh 1996)

$$C_1 = \frac{\Delta h_{T_r} + a'(\cos\alpha)_{T_r} + b(\cos\alpha)_{T_r}T_r}{T_r} \tag{12}$$

To better illustrate the effects of temperature on contact angle, Fig. 3 depicts matric suction versus pore size at different temperatures ranging from 25 to 100°C for two cases: (1) temperature-independent contact angle (black solid lines), generated by substituting Eqs. (6) and (7) into Eq. (4); and (2) temperature-dependent contact angle (red dashed lines), generated by implementing Eqs. (6), (7), (9), (11), and (12) into Eq. (4). For plotting the temperature-dependent contact angle results, $\Delta h_{(T_r)}$ is assumed to be -0.516 J/m^2, which is reported for silt by Grant and Salehzadeh (1996). The results are shown for a wide range of pore size representing various soil types. For example, Nimmo (2004) reports the following typical r values for different soils: very coarse sand, 1.5 mm; coarse sand, 0.75 mm; fine sand, 0.175 mm; very fine sand, 0.075 mm; silt, 0.02 mm; and clay, 0.0015 mm.

As shown in Fig. 3 using the black solid lines, changes in matric suction for the temperature-independent contact angle are not significant. For example, for $r = 0.6$ mm the matric suction decreases as much as 12% by increasing temperature from 25 to 100°C. However, using the temperature-dependent contact angle can lead to significantly larger reductions in matric suction by increasing temperature. For $r = 0.6$ mm, the matric suction decreases approximately by 40, 47, 63, and 82% by increasing the temperature from 25 to 40, 60, 80, and 100°C, respectively. Comparison between the results from the two cases examined demonstrates that accounting for the effects of temperature only on surface tension is not enough to evaluate the SWRC under nonisothermal conditions. The results highlight the importance of considering a temperature-dependent contact angle for multiphysics numerical simulations involving nonisothermal processes in unsaturated soils. This aspect is commonly overlooked in the majority of previous nonisothermal simulations.

Temperature-Dependent Function for Matric Suction

If the wetting coefficient and the surface tension are considered as functions of temperature, Grant and Salehzadeh (1996) showed that Eq. (5) could be rewritten as

$$\frac{\psi}{\left(\frac{\partial\psi}{\partial T}\right)} = \beta(T) + T \tag{13}$$

where $\beta(T) = \frac{-\Delta h}{C_1}$. By separation of variables and integration, Eq. (13) leads to the following closed-form expression for nonisothermal matric suction that can be incorporated into any SWRC model:

$$\psi = \psi_{T_r}\left(\frac{\beta + T}{\beta_{T_r} + T_r}\right) \tag{14}$$

where ψ_{T_r} = matric suction at the reference temperature.

Nonisothermal Extension of SWRC Models

The proposed formulations for the temperature-dependent adsorbed water [Eq. (5)] and the temperature-dependent matric suction [Eq. (14)] can be readily incorporated into existing isothermal SWRCs to extend them to nonisothermal conditions. The following sections demonstrate the extension of three widely used SWRC models originally developed by Brooks and Corey (1964) (referred to as BC), van Genuchten (1980) (referred to as VG), and Fredlund and Xing (1994) (referred to as FX) to nonisothermal conditions. Further discussion about the characteristics of each of the original models, including their advantages and limitations, can be found in the literature (e.g., Fredlund et al. 2011).

Table 1. Parameters for nonisothermal extension of SWRC models

	General parameters					Model-specific parameters		
Soil	θ_s	θ_r	$\Delta h_{(T_r)}$ (J/m^2)	T_r (K)	M	Brooks and Corey (1964)	van Genuchten (1980)	Fredlund and Xing (1994)
Ottawa sand	0.4	0.017	−0.285	298	0.789	$\lambda = 1.7341$ $p^b = 2.5107$ kPa	$m_{VG} = 0.789$ $n_{VG} = 4.504$ $\alpha_{VG} = 0.282$ kPa^{-1}	$m_{FX} = 1.551$ $n_{FX} = 4.692$ $a_{FX} = 3.33$ kPa
Wyoming bentonite	0.7	0.217	−0.516	298	0.047	$\lambda = 0.46161$ $p^b = 591.72$ kPa	$m_{VG} = 0.047$ $n_{VG} = 9.667$ $\alpha_{VG} = 0.002$ kPa^{-1}	$m_{FX} = 0.634$ $n_{FX} = 0.976$ $a_{FX} = 200$ kPa

J. Geotech. Geoenviron. Eng., 2018, 144(9): 04018061

The three SWRC models examined in this study, as well as the majority of other existing SWRC models in the literature, are empirical, primarily relying upon fitting parameters to simulate the measured SWRC data. Some of these fitting parameters (e.g., air-entry suction, pore-size distribution) can be evidently attributed to their pertinent physical interpretations. However, some other fitting parameters (e.g., residual water content, and residual suction) are not clearly defined and physically interpreted (Lu 2016). In this study, the residual water content is considered to correspond to the adsorbed water, as suggested by Revil and Lu (2013). The latter consideration allows to distinctly determine the adsorption water and capillary water, which are not explicitly distinguished in the original SWRC models used in the current study.

The extended SWRC models are used to show adsorbed water, capillary water, and total water content versus matric suction for Ottawa sand and Wyoming bentonite subjected to several temperatures ranging from 25 to 100°C. These temperatures and soil types are selected to illustrate the impact of temperature on the SWRC for a wide range of suction and applications. The upper limit of 100°C is chosen because this temperature is imposed unanimously in the majority of nuclear waste disposal design methods (Hicks et al. 2009). Table 1 shows the parameters that are used for nonisothermal extension of the SWRC models in the rest of this section. Except for the term $\Delta h_{(T_r)}$, which is taken from Grant and Salehzadeh (1996), the rest of the parameters for the VG and FX models are obtained from those reported in Lu (2016) and the BC model parameters are obtained using the nonlinear fitting program by Seki (2007). Following Revil and Lu (2013), the adsorption strength, M, for each model/soil is estimated to be equal to the shape fitting parameter for the SWRC of VG model.

Brooks and Corey

For suctions greater than the air-entry suction, Brooks and Corey (1964) presented the following SWRC:

$$\theta = \theta_r + (\theta_s - \theta_r)\left(\frac{p^b}{\psi}\right)^{\lambda} \tag{15}$$

where θ_s = saturated water content; θ_r = residual water content; p^b = bubbling pressure in kPa; and λ = pore size distribution index. We extend the BC model to nonisothermal conditions by replacing the residual water content with the adsorbed water [Eq. (3)] and using the temperature-dependent matric suction [Eq. (14)]. Consequently, the nonisothermal SWRC of Brooks and Corey (1964) can be written as follows:

$$\theta = \theta_a + (\theta_s - \theta_a)\left(\frac{p^b}{\psi_{T_r}}\right)^{\lambda} \tag{16}$$

The full expression of the nonisothermal SWRC of the BC model can be written as

$$\theta = \theta_a^{\max}\left[\exp\left(-\frac{M_w\psi}{RT}\right)\right]^{1/M} + \left\{\theta_s - \theta_a^{\max}\left[\exp\left(-\frac{M_w\psi}{RT}\right)\right]^{1/M}\right\}\left[\frac{p^b}{\psi\left(\frac{\beta_{T_r}+T_r}{\beta+T}\right)}\right]^{\lambda} \tag{17}$$

To illustrate the performance of the new BC model, Figs. 4 and 5 show the temperature effects on SWRCs for Ottawa sand and Wyoming bentonite, respectively. For Ottawa sand, Figs. 4(a–c) illustrate the changes in the adsorbed, capillary, and total water contents at different temperatures (25–100°C), respectively. The matric suction primarily varies between 0 and 10 kPa, a low matric suction range where the capillary water dominates and the adsorbed water contribution is minimal. To better understand the effects of temperature, we further examine the changes in each water component by temperature at the matric suction of 5 kPa. As shown in Fig. 4(b), the capillary water decreases approximately by 16, 50, 68 and 84%, [Fig. 4(b)] by increasing the temperature from 25 to 40, 60, 80, and

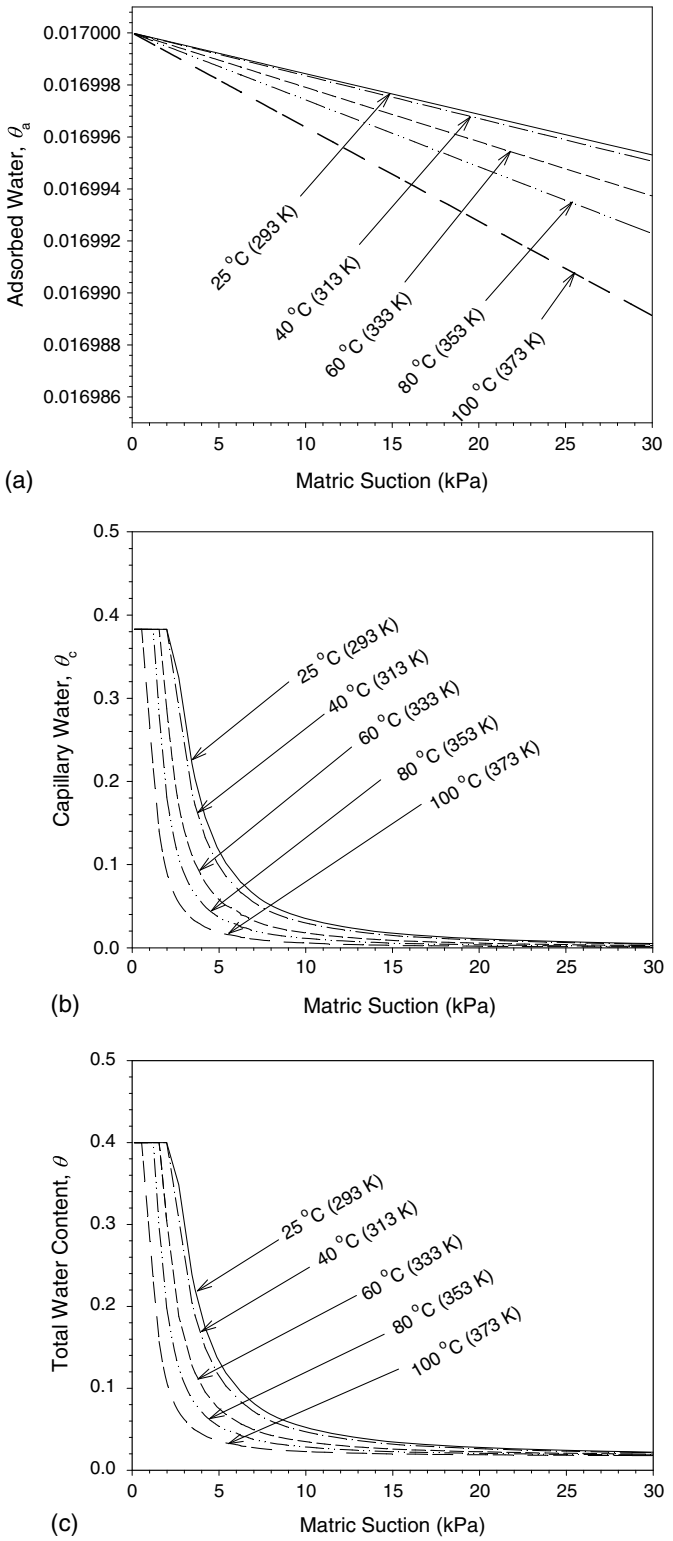

Fig. 4. Nonisothermal extension of the Brooks and Corey (1964) SWRC for Ottawa sand at different temperatures: (a) adsorbed water; (b) capillary water; and (c) total water content.

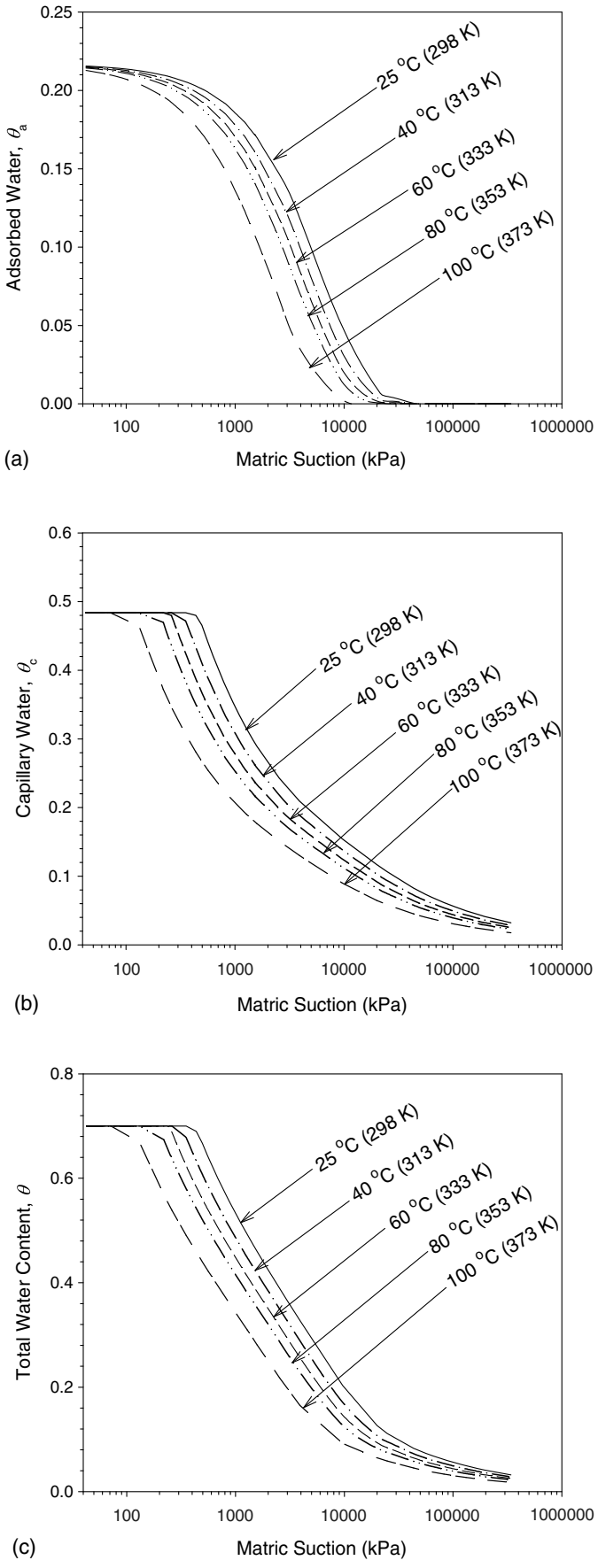

Fig. 5. Nonisothermal extension of the Brooks and Corey (1964) SWRC for Wyoming bentonite at different temperatures: (a) adsorbed water; (b) capillary water; and (c) total water content.

100°C, respectively, due to changes in surface tension and enthalpy. However, the maximum reduction in the adsorbed water [Fig. 4(a)] is less than 1% when increasing the temperature from 25 to 100°C. Consequently, the reduction in the total water content [Fig. 4(c)] is primarily dominated by the changes in the capillary water.

For Wyoming bentonite, Fig. 5 reveals that both the capillary water and the adsorbed water have considerable contributions to the total water content. Further, the results demonstrate the significant impact of temperature on capillary and the adsorbed waters. For example, at matric suction of 1,500 kPa, the reduction in the capillary water [Fig. 5(b)] between the room temperature (25°C) and at 40, 60, 80, and 100°C is approximately 11, 19, 26 and 39%, respectively. The reduction in the adsorbed water [Fig. 5(a)] between the room temperature (25°C) and at 40, 60, 80, and 100°C is approximately 6, 12, 18 and 37%, respectively. The effects of temperature increases as the matric suction increases because the adsorption dominates at higher suctions. The results of both soils suggest that increases in temperature lead to smaller air-entry matric suctions. This observation can assist for more realistic simulations of nonisothermal problems in unsaturated soils.

van Genuchten

The van Genuchten (1980) equation is one of the most commonly used SWRC models. The VG model can be written as

$$\theta = \theta_r + (\theta_s - \theta_r)[1 + (\alpha_{VG}\psi)^{n_{VG}}]^{-m_{VG}} \tag{18}$$

where α_{VG} = fitting parameter inversely related to the air-entry suction (1/kPa); n_{VG} = pore-size distribution fitting parameter; and m_{VG} = fitting parameter representing the overall geometry of the SWRC. Similar to the aforementioned procedure used for the BC model, a new model for the nonisothermal version of the VG model can be written as follows:

$$\theta = \theta_r + (\theta_s - \theta_r)[1 + (\alpha_{VG}\psi_{T_r})^{n_{VG}}]^{-m_{VG}} \tag{19}$$

The full expression of nonisothermal version of the SWRC of the VG model is

$$\theta = \theta_a^{\max}\left[\exp\left(-\frac{M_w\psi}{RT}\right)\right]^{1/M} + \left\{\theta_s - \theta_a^{\max}\left[\exp\left(-\frac{M_w\psi}{RT}\right)\right]^{1/M}\right\} \times \left\{1 + \left[\alpha_{VG}\psi\left(\frac{\beta_{T_r} + T_r}{\beta + T}\right)\right]^{n_{VG}}\right\}^{-m_{VG}} \tag{20}$$

Figs. 6 and 7 show the temperature effects on the VG model for Ottawa sand and Wyoming bentonite, respectively. The SWRCs sensitivity to temperature shows a similar trend that presented in Figs. 4 and 5. For Ottawa sand, at the matric suction of 5 kPa, the capillary water decreases approximately by 27, 74, 90, and 97% by increasing the temperature from 25 to 40, 60, 80, and 100°C, respectively. The reduction in the adsorbed water is identical to the BC model.

For Wyoming bentonite, at matric suction of 1,500 kPa, the reduction in the capillary water [Fig. 7(b)] between the room temperature (25°C) and at 40, 60, 80, and 100°C is approximately 11, 19, 26, and 38%, respectively. The reduction in the adsorbed water [Fig. 7(a)] between the room temperature (25°C) and at 40, 60, 80, and 100°C is approximately 6, 12, 18, and 37%, respectively. It is noted that the effect of temperature on the SWRC is more pronounced in the extended VG model compared to the nonisothermal BC model, leading to sharper reductions in water content by increasing temperature.

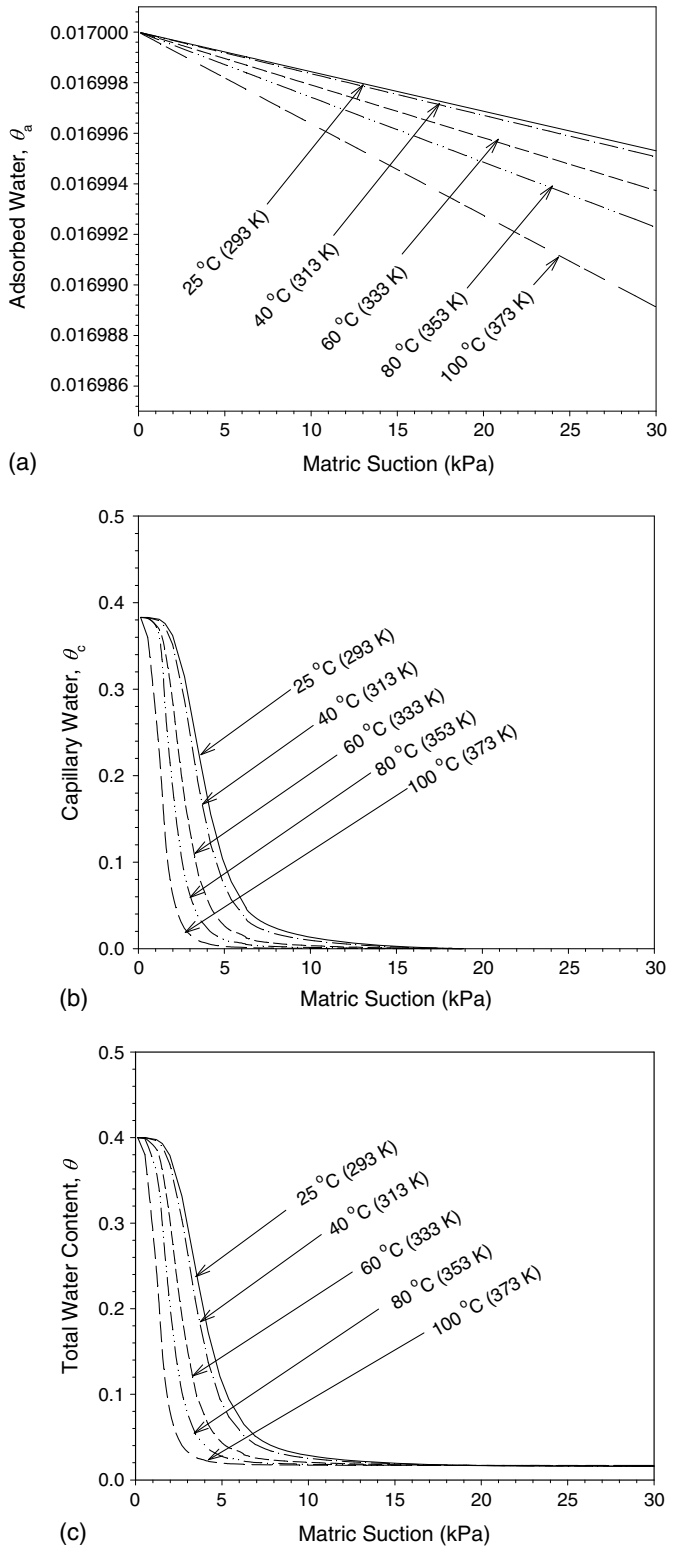

Fig. 6. Nonisothermal extension of the van Genuchten (1980) SWRC for Ottawa sand at different temperatures: (a) adsorbed water; (b) capillary water; and (c) total water content.

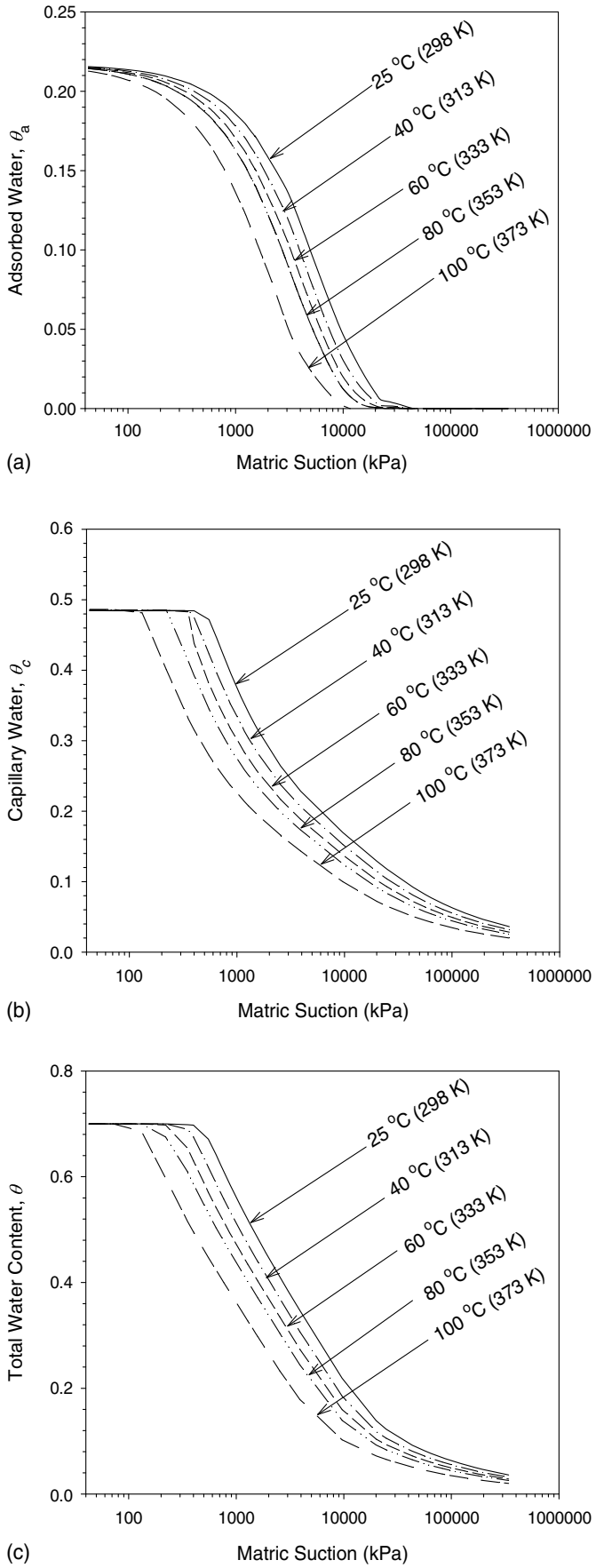

Fig. 7. Nonisothermal extension of the van Genuchten (1980) SWRC for Wyoming bentonite at different temperatures: (a) adsorbed water; (b) capillary water; and (c) total water content.

Fredlund and Xing

Fredlund and Xing (1994) proposed a SWRC model that provides a steady and continuous function, which is valid for a wider range of suction compared to the two previously mentioned SWRC models (e.g., Leong and Rahardjo 1997; Stormont and Anderson 1999;

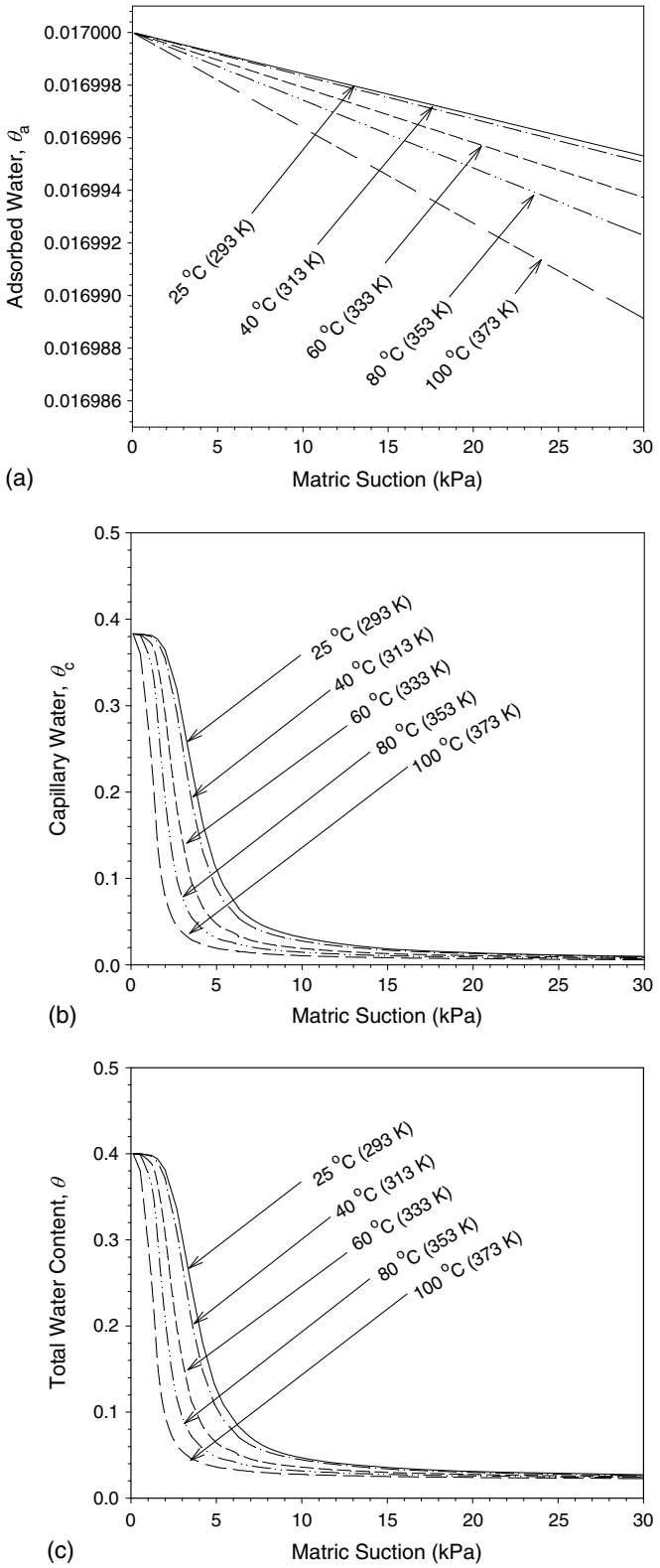

Fig. 8. Nonisothermal extension of the Fredlund and Xing (1994) SWRC for Ottawa sand at different temperatures: (a) adsorbed water; (b) capillary water; and (c) total water content.

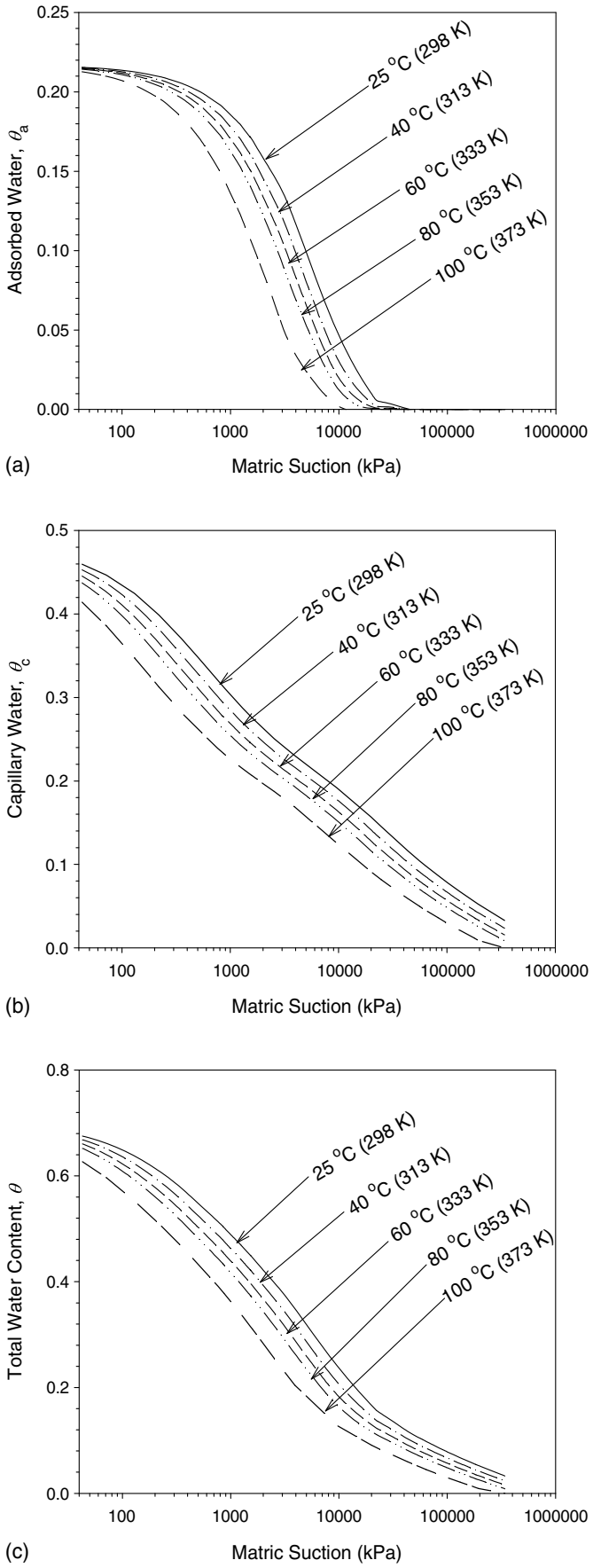

Fig. 9. Nonisothermal extension of the Fredlund and Xing (1994) SWRC for Wyoming bentonite at different temperatures: (a) adsorbed water; (b) capillary water; and (c) total water content.

Fredlund et al. 2011; Gerscovich and Sayao 2002). In this study, the FX model with correction factor, $C(\psi)$, is used for extension to nonisothermal conditions. The correction factor extends the range of suctions beyond the residual suction to completely dry

Table 2. Model parameters for the proposed nonisothermal extension of the Fredlund and Xing (1994) SWRC

Type of soil	Parameters						
	θ_s	n_{FX}	m_{FX}	a_{FX} (kPa)	ψ_r (MPa)	$\Delta h_{(T_r)}$ (J/m^2)	T_r (K)
GMZ01 bentonite	0.67	0.8086	0.5864	8.0×10^3	309	−0.516	293
Superfine sand	0.39	6.615	0.8488	4.6	3.0	−0.285	293
Bourke silt	0.55	1.393	0.9814	55	1.5	−0.516	298

conditions. The isothermal FX model with the correction factor can be written as

$$\theta = \theta_r + (\theta_s - \theta_r)C(\psi)\left\{\ln\left[e + \left(\frac{\psi}{a_{FX}}\right)^{n_{FX}}\right]\right\}^{-m_{FX}} \tag{21}$$

and the correction factor is defined as

$$C(\psi) = 1 - \frac{\ln\left(1 + \frac{\psi}{\psi_r}\right)}{\ln\left(1 + \frac{\psi_{\max}}{\psi_r}\right)} \tag{22}$$

where ψ_r = matric suction corresponding to the residual water content commonly set to be 1,500 kPa; $\psi_{\max}$ = highest matric suction (kPa) corresponding to zero water content, commonly set to be 10^6 kPa; n_{FX} = fitting parameter related to pore size distribution; m_{FX} = fitting parameter controlling the overall geometry of the SWRC; and a_{FX} = fitting parameter related to the air-entry suction. Similar to the procedures explained previously, the nonisothermal version of the FX model is written

$$\theta = \theta_r + (\theta_s - \theta_a)\left[1 - \frac{\ln\left(1 + \frac{\psi_{T_r}}{\psi_r}\right)}{\ln\left(1 + \frac{\psi_{\max}}{\psi_r}\right)}\right]\left\{\ln\left[e + \left(\frac{\psi_{T_r}}{a_{FX}}\right)^{n_{FX}}\right]\right\}^{-m_{FX}} \tag{23}$$

The full expression of the nonisothermal FX model can be written

$$\theta = \theta_a^{\max}\left[\exp\left(-\frac{M_w\psi}{RT}\right)\right]^{1/M} + \left\{\theta_s - \theta_a^{\max}\left[\exp\left(-\frac{M_w\psi}{RT}\right)\right]^{1/M}\right\} \times \left\{1 - \frac{\ln\left[1 + \frac{\psi\left(\frac{\beta_{T_r} + T_r}{\beta + T}\right)}{\psi_r}\right]}{\ln\left(1 + \frac{\psi_{\max}}{\psi_r}\right)}\right\}\left\{\ln\left[e + \left(\frac{\psi\left(\frac{\beta_{T_r} + T_r}{\beta + T}\right)}{a_{FX}}\right)^{n_{FX}}\right]\right\}^{-m_{FX}} \tag{24}$$

Figs. 8 and 9 show the temperature effects on the FX model for Ottawa sand and Wyoming bentonite, respectively. The SWRC sensitivity to temperature shows a similar trend to that presented in Figs. 6 and 7. For Ottawa sand, we further examine the changes in each water component at the matric suction of 5 kPa. As shown in Fig. 8(b), the capillary water decreases approximately by 19, 55, 70, and 81% by increasing the temperature from 25 to 40, 60, 80, and 100°C, respectively. The reduction in adsorbed water is negligible likewise the BC and VG models. For Wyoming bentonite, at matric suction of 1,500 kPa, the reduction in the total water content [Fig. 9(c)] between the room temperature (25°C) and at 40, 60, 80, and 100°C is approximately 6, 11, 16, and 25%, respectively.

Comparison to Experimental Test Results

The proposed nonisothermal extension of the FX model is compared against three independent sets of experimental test results reported in the literature for clay (Wan et al. 2015), sand (Roshani and Sedano 2016), and silt (Uchaipichat and Khalili 2009). Similar comparisons for the other proposed nonisothermal SWRC models can be performed upon availability of all the required input parameters. The accuracy of the nonisothermal SWRC model is evaluated by the root-mean square error (RMSE) between the predicted and measured water contents using

$$\text{RMSE} = \sqrt{\frac{\sum(\theta_{measured} - \theta_{predicted})^2}{N}} \tag{25}$$

where $\theta_{measured}$ = measured (volumetric) total water content from experiment; $\theta_{predicted}$ = predicted (volumetric) total water content from the nonisothermal SWRC; and N = number of measured data points. Table 2 shows the fitting parameters used for the proposed FX model for the soils that are examined. All of the experimental test results used for comparison purposes only report capillary water at various temperatures. Consequently, the contribution of the adsorbed water is not included in the calculation of the total water content in the following sections (i.e., $\theta_a = 0$).

Comparison for Clay

Wan et al. (2015) performed a set of SWRC tests on GMZ01 bentonite samples at temperatures of 20°C (293 K), 40°C (313 K), and 60°C (333 K). For controlling suction at a given temperature, Wan et al. (2015) used two techniques: (1) vapor equilibrium technique (controlling total suction), which is based on the use of polyethylene glycol solutions, and (2) osmotic technique (controlling matric suction), which is based on the use of salt solutions (e.g., $LiCl_2$, $MgCl_2$, NaCl, KCl). They used the osmotic technique and vapor equilibrium technique for low matric suctions (<1.5 MPa) and

Table 3. Properties of GMZ01 bentonite

Soil property	Description
Specific gravity of soil grain	2.66
Dry density (g/cm^3)	1.7
pH	8.68–9.86
Liquid limit (%)	276
Plastic limit (%)	37
Total specific surface area (m^2 g^{-1})	570
Cation exchange capacity (mmol g^{-1})	0.7730
Main exchanges cation (mmol g^{-1})	Na^+ (0.433 6), Ca^{2+} (0.291 4), Mg^{2+} (0.123 3), K^+ (0.025 1)
Main minerals	Montmorillonite (75.4%), quartz (11.7%), feldspar (4.3%), cristobalite (7.3%)

Source: Data from Ye et al. (2012).

J. Geotech. Geoenviron. Eng., 2018, 144(9): 04018061

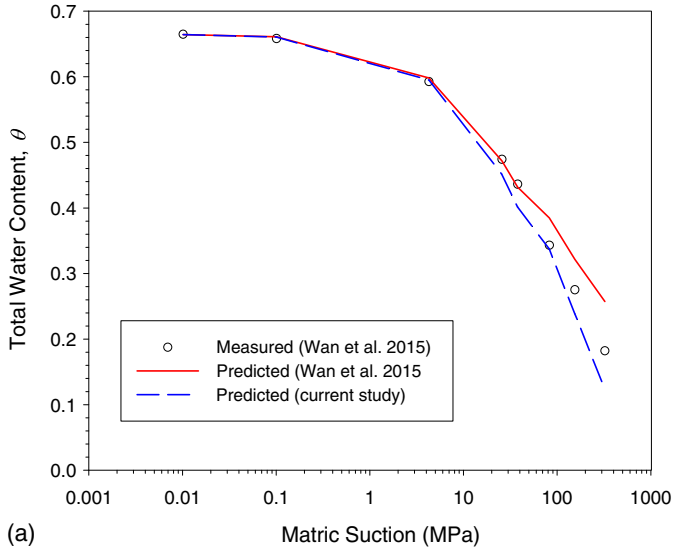

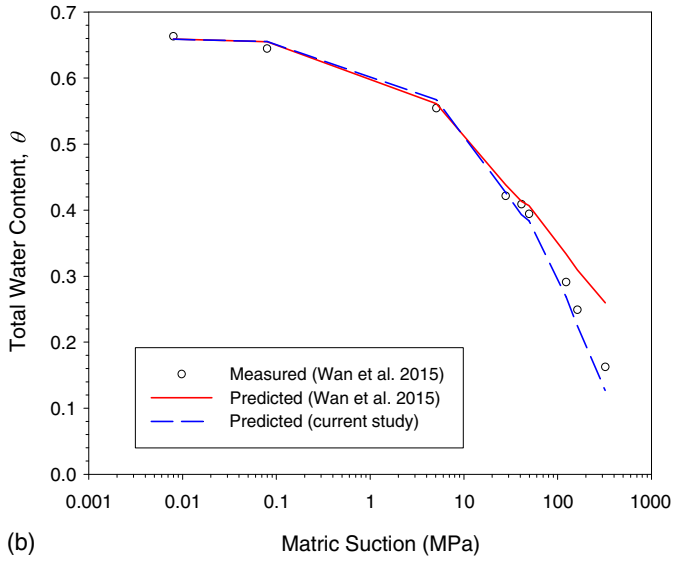

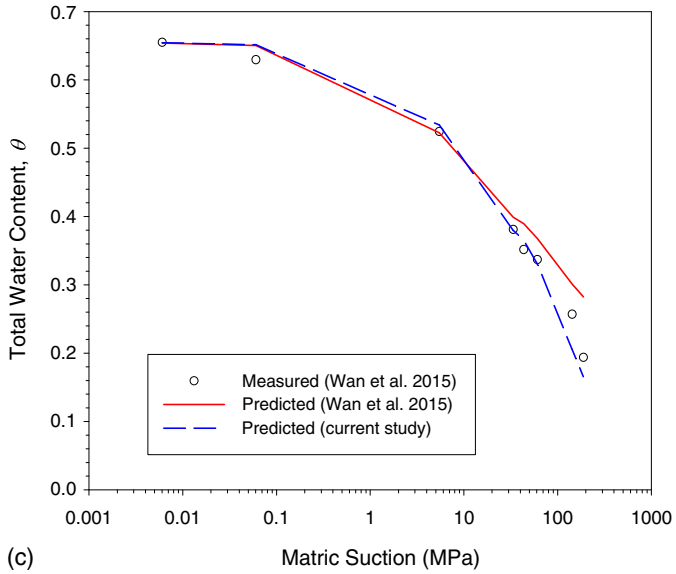

Fig. 10. Predicated and measured SWRCs for GMZ01 bentonite: (a) at T = 20°C (293 K); (b) at T = 40°C (313 K); (c) at T = 60°C (333 K).

higher suctions (>1.5 MPa), respectively. Table 3 shows the properties of GMZ01 bentonite (Ye et al. 2012).

Fig. 10 compares the measured values versus predictions of the proposed FX model at 20°C (293 K), 40°C (313 K), and 60°C (333 K). The results are also compared against the predicted SWRC by Wan et al. (2015). The comparison shows that the results obtained from the proposed FX model are in closer agreement with the experimental results. As expected, at the same matric suction level, the water content decreases with increase in temperature. The temperature effect is insignificant at low suctions but the effect becomes more pronounced as the suction increases because the adsorption dominates at higher suctions. At temperatures of 20°C (293 K), 40°C (313 K), and 60°C (333 K), the RMSE values for the predicted SWRC by Wan et al. (2015) are calculated as 1.3, 1.6, and 1.5% respectively. For the extended FX model, the calculated RMSE values are 1.1, 0.7 and 0.9%, respectively.

The main differences between the proposed nonisothermal FX model and the nonisothermal SWRC model of Wan et al. (2015) are: (1) Wan et al. (2015) assumed that the surface tension is the only temperature-dependent parameter and derived the expression by modifying the a parameter with respect to temperature in the FX model; and (2) in the current study, the SWRC model is derived by considering the influence of temperature on adsorption, contact angle and surface tension.

Comparisons for Sand

The proposed nonisothermal FX model is compared against the SWRC experimental test results reported by Roshani and Sedano (2016). The tests are conducted on superfine sand (finer than #35 mesh, 0.5 mm) at temperatures of 4°C (277 K), 20°C (293 K), and 49°C (322 K). For controlling the suction at a given temperature, Roshani and Sedano (2016) used the axis translation technique with Tempe cell. Table 4 shows the properties of superfine sand tested by Roshani and Sedano (2016).

Fig. 11 compares the SWRC obtained from the proposed FX model against measured and predicted SWRCs by Roshani and Sedano (2016) at various temperatures. As can be seen in Fig. 11, the results obtained from the proposed FX model are in closer agreement with the experimental data than the Roshani and Sedano (2016) model. For the Roshani and Sedano model (2016), the RMSE values are calculated to be 8.85, 6.82, and 5.33% at 4°C (277 K), 20°C (293 K), and 49°C (322 K), respectively, whereas for the proposed extended FX model, the calculated RMSE values are 4.7, 2.5, and 3.0%, respectively. Overall, the proposed model shows good agreement with the measured data at both lower and higher suction ranges.

The proposed model predicts better than the Roshani and Sedano (2016) model in low suctions, where the capillary water controls

Table 4. Properties of super fine sand

Soil property	Description
Specific gravity (G_s)	2.65
Optimum moisture content (%)	14.6
Maximum dry unit weight (kN/m^3)	16.8
Void ratio (e)	0.63
D_{60} (mm)	0.22
D_{30} (mm)	0.18
D_{10} (mm)	0.12
Coefficient of uniformity, C_u	1.83
Coefficient of curvature, C_c	1.23

Source: Data from Roshani and Sedano (2016).

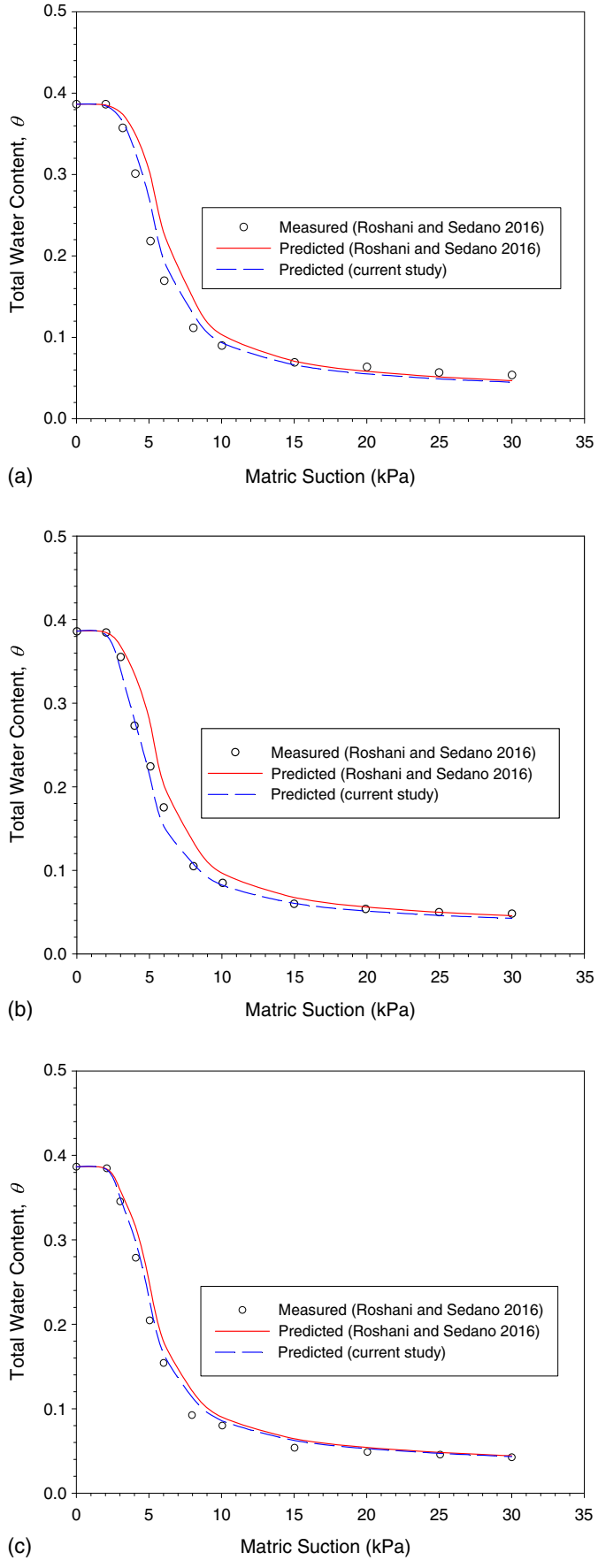

Fig. 11. Predicated and measured SWRCs for super fine sand: (a) at T = 4°C (277 K); (b) at T = 20°C (293 K); and (c) at T = 49°C (322 K).

Table 5. Properties of Bourke silt

Soil property	Description
Liquid limit (%)	20.5
Plastic limit (%)	14.5
Specific gravity	2.65
Maximum dry unit weight (kN/m^3)	18.8
Optimum moisture content (%)	12.5

Source: Data from Uchaipichat and Khalili (2009).

changes in the water content. However, as illustrated in Fig. 11, both models predict nearly the same at high suctions. The differences in the models at low suctions can be explained by the fact that by increasing the temperature the pores are almost in the dry state, and the binding of the water is not caused by capillary forces but by adsorptive forces. Hence, the temperature-dependency of enthalpy has more significance, which is only incorporated in the proposed model.

Comparison for Silt

Uchaipichat and Khalili (2009) performed a set of SWRC tests on silt specimens by using a modified Bishop–Wesley triaxial cell and used the axis translation technique for controlling the suction at temperatures of 25°C (298 K), 40°C (313 K), and 60°C (333 K). The tests were performed on silt obtained from the Bourke region of New South Wales, Australia. Table 5 shows the properties of Bourke silt tested by Uchaipichat and Khalili (2009).

Fig. 12 compares the predictions of the extended FX model at temperatures of 25°C (298 K), 40°C (313 K), and 60°C (333 K) with the measured SWRC by Uchaipichat and Khalili (2009). The results obtained from the proposed model are in very good agreement with the experimental results. Unlike many of the existing nonisothermal SWRC models, the proposed model captures the decrease in the adsorbed water with temperature, which is observed in the experimental data. At temperatures of 25°C (298 K), 40°C (313 K), and 60°C (333 K), the RMSE values for the proposed FX model are 1.0, 1.1, and 1.1%, respectively.

Conclusions

Several emerging issues and applications in geotechnical and geoenvironmental engineering necessitate the knowledge of nonisothermal behavior of unsaturated soils. A key constitutive relationship for this purpose is the nonisothermal soil water retention curve (SWRC). In this study, the effects of temperature were incorporated into the SWRC by considering thermal effects on the adsorbed water, the contact angle, and the surface tension of water. Previous nonisothermal SWRC models do not consider all these effects together and commonly fail to account for the effect of temperature in the adsorption regime, which can be significant at higher matric suctions. This paper presented analytical formulations for temperature-dependent adsorbed water and matric suction developed based upon fundamental physics of adsorption and wettability. The proposed formulations were then used to extend three isothermal SWRC models of Brooks and Corey (1964), van Genuchten (1980), and Fredlund and Xing (1994) to nonisothermal conditions.

The proposed formulations can be readily incorporated into analytical solutions and numerical simulations of thermo-hydro-mechanical processes in unsaturated soils. The effects of temperature vary based upon various parameters including soil type, soil mineralogy, range of temperature, range of suction, saturation

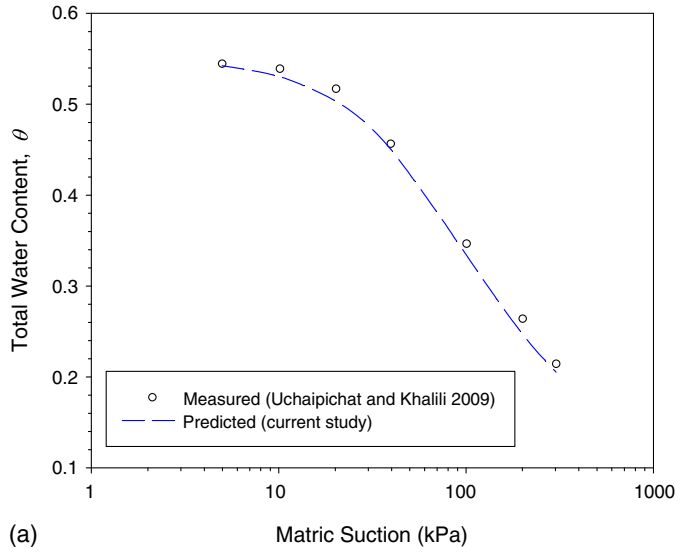

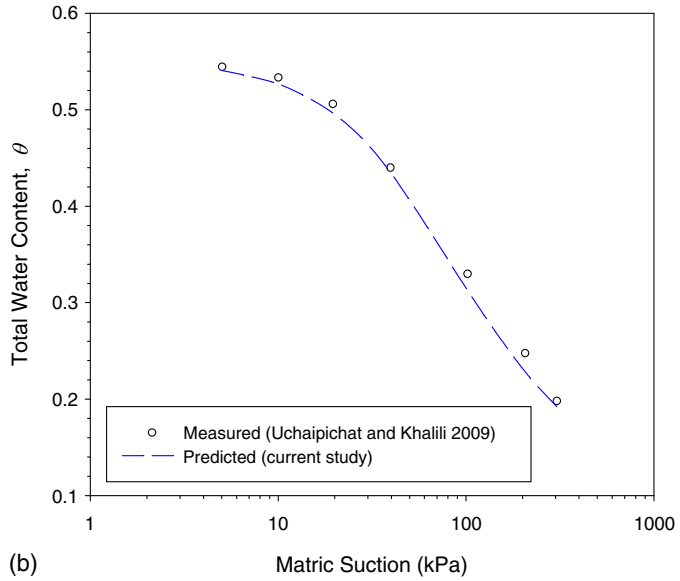

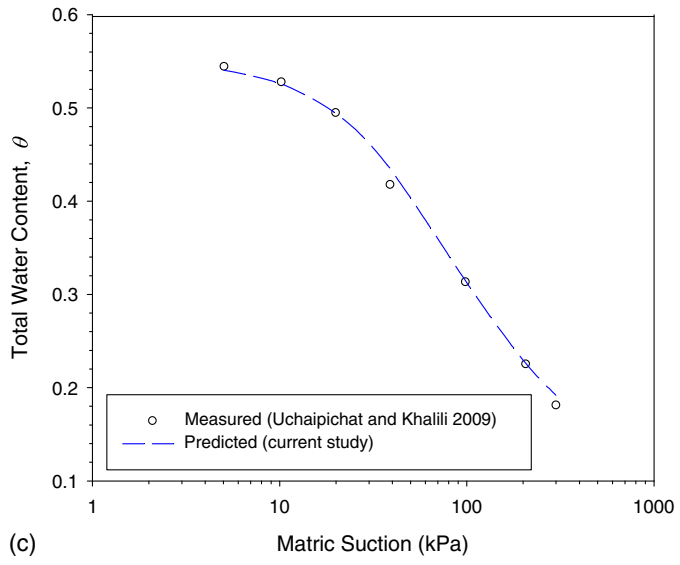

Fig. 12. Predicated and measured SWRCs for Bourke silt: (a) at T = 25°C (298 K); (b) at T = 40°C (313 K); and (c) at T = 60°C (333 K).

levels, soil confinement, among others. The current study showed that, temperature effects on the SWRCs can be significant, particularly for fine-grained soils subjected to high temperatures (e.g., >60°C). Several nonisothermal applications, such as nuclear waste disposal, radioactive barriers, and buried high-voltage cables, can present temperatures as high as 100°C or even more. Considering a nonisothermal SWRC is prudent for such high temperatures, further highlighting the applied character of this study.

Acknowledgments

This material is based upon work supported in part by the National Science Foundation under Grant No. CMMI-1634748. Any opinions, findings, and conclusions or recommendations expressed in this material are those of the authors and do not necessarily reflect the views of the National Science Foundation.

References

Alsherif, N. A., and J. S. McCartney. 2015. "Nonisothermal behavior of compacted silt at low degrees of saturation." *Géotechnique* 65 (9): 703–716. https://doi.org/10.1680/geot.14.P.049.

Bachmann, J., R. Horton, S. A. Grant, and R. R. van der Ploeg. 2002. "Temperature dependence of water retention curves for wettable and water-repellent soils." *Soil Sci. Soc. Am. J.* 66 (1): 44–52. https://doi.org/10.2136/sssaj2002.4400.

Brooks, R. H., and A. T. Corey. 1964. *Hydraulic properties of porous media: Hydrology paper No. 3*. Fort Collins, CO: Colorado State Univ.

Coccia, C. J. R., and J. S. McCartney. 2012. "A thermo-hydro-mechanical true triaxial cell for evaluation of the impact of anisotropy on thermally-induced volume changes in soils." *ASTM Geotech. Test. J.* 35 (2): 227–237. https://doi.org/10.1520/GTJ103803.

Derjaguin, B. V., V. V. Karasev, and E. N. Khromova. 1986. "Thermal expansion of water in fine pores." *J. Colloid Interface Sci.* 109 (2): 586–587. https://doi.org/10.1016/0021-9797(86)90340-1.

Dorsey, N. E. 1940. *Properties of ordinary water substance*. New York: Reinhold.

Everett, D. H. 1972. "Definitions, terminology and symbols in colloid and surface chemistry." *Pure Appl. Chem.* 31 (4): 577–638.

François, B., and S. Ettahiri. 2012. "Role of the soil mineralogy on the temperature dependence of the water retention curve." In Vol. 1 of *Unsaturated soils: Research and application, 2nd European Conf. on Unsaturated Soils (E-UNSAT)*, 173–178. Berlin: Springer.

Fredlund, D. G., D. Sheng, and J. Zhao. 2011. "Estimation of soil suction from the soil-water characteristic curve." *Can. Geotech. J.* 48 (2): 186–198. https://doi.org/10.1139/T10-060.

Fredlund, D. G., and A. Xing. 1994. "Equations for the soil-water characteristic curve." *Can. Geotech. J.* 31 (4): 521–532. https://doi.org/10.1139/t94-061.

Gerscovich, D. M. S., and A. S. F. J. Sayão. 2002. "Evaluation of soil–water characteristic curves for soils from Brazil." In *Proc., 3rd Int. Conf. on Unsaturated Soils*, edited by J. F. T. Juca, T. M. P. de Campos, and F. A. M. Marinho, 295–300. Lisse, Netherlands: Swets & Zeitlinger.

Grant, S. A., and A. Salehzadeh. 1996. "Calculation of temperature effects on wetting coefficients of porous solids and their capillary pressure functions." *Water Resour. Res.* 32 (2): 261–270. https://doi.org/10.1029/95WR02915.

Haar, L., J. S. Gallagher, and G. S. Kell. 1984. *NBS/NRC steam table*. New York: Hemisphere Publishing Corporation.

Harkins, W. D., and G. Jura. 1944. "Surfaces of solids. XII. An absolute method for the determination of the area of a finely divided crystalline solid." *J. Am. Chem. Soc.* 66 (8): 1362–1366. https://doi.org/10.1021/ja01236a047.

Hicks, T. W., M. J. White, and P. J. Hooker. 2009. *Role of bentonite in determination of thermal limits on geological disposal facility design*. Rep. 0883–1, Version 2. Rutland, UK: Falson Sciences Ltd.

Imbert, C., E. Olchitzky, T. Lassabatere, P. Dangla, and A. Courtois. 2005. "Evaluation of a thermal criterion for an engineered barrier system." *Eng. Geol.* 81 (3): 269–283. https://doi.org/10.1016/j.enggeo.2005.06.019.

Jacinto, A. C., M. V. Villar, R. Gómez-Espina, and A. Ledesma. 2009. "Adaptation of the van Genuchten expression to the effects of temperature and density for compacted bentonites." *Appl. Clay Sci.* 42 (3): 575–582. https://doi.org/10.1016/j.clay.2008.04.001.

Jeppu, G. P., and T. P. Clement. 2012. "A modified Langmuir-Freundlich isotherm model for simulating pH-dependent adsorption effects." *J. Contam. Hydrol.* 129 (3): 46–53. https://doi.org/10.1016/j.jconhyd.2011.12.001.

Khorshidi, M., N. Lu, I. D. Akin, and W. J. Likos. 2016. "Intrinsic relation between specific surface area and soil water retention." *J. Geotech. Geoenviron. Eng.* 143 (1): 04016078. https://doi.org/10.1061/(ASCE)GT.1943-5606.0001572.

Lebeau, M., and J.-M. Konrad. 2010. "A new capillary and thin film flow model for predicting the hydraulic conductivity of unsaturated porous media." *Water Resour. Res.* 46 (12): W12554 https://doi.org/10.1029/2010WR009092.

Leong, E. C., and H. Rahardjo. 1997. "Permeability functions for unsaturated soils." *J. Geotech. Geoenviron. Eng.* 123 (12): 1118–1126. https://doi.org/10.1061/(ASCE)1090-0241(1997)123:12(1118).

Lu, N. 2016. "Generalized soil water retention equation for adsorption and capillarity." *J. Geotech. Geoenviron. Eng.* 142 (10): 04016051. https://doi.org/10.1061/(ASCE)GT.1943-5606.0001524.

Lu, N., and W. J. Likos. 2004. *Unsaturated soil mechanics*. Hoboken, NJ: Wiley.

Ma, C., and T. Hueckel. 1992. "Stress and pore pressure in saturated clay subjected to heat from radioactive, waste: A numerical simulation." *Can. Geotech. J.* 29 (6): 1087–1094. https://doi.org/10.1139/t92-125.

McCartney, J. S., C. J. R. Coccia, N. Alsherif, and M. A. Stewart 2013. "Energy geostructures in unsaturated soils." Chap. 5 in *Energy geostructures: Innovation in underground engineering*, edited by L. Laloui and A. DiDonna, 99–114. Hoboken, NJ: Wiley-ISTE.

McQueen, I. S., and R. F. Miller. 1974. "Approximating soil moisture characteristics from limited data: Empirical evidence and tentative model." *Water Resour. Res.* 10 (3): 521–527. https://doi.org/10.1029/WR010i003p00521.

Mitchell, J. K., and K. Soga. 2005. *Fundamentals of soil behavior*. 3rd ed. New York: Wiley.

Nimmo, J. R. 2004. "Porosity and pore size distribution." In Vol. 3 of *Encyclopedia of soils in the environment*, edited by D. Hillel, 295–303. London: Elsevier.

Philip, J. R., and D. A. de Vries. 1957. "Moisture movement in porous materials under temperature gradients." *AGU Trans.* 38 (2): 222–232. https://doi.org/10.1029/TR038i002p00222.

Ponec, V., Z. Knor, and S. Cerny. 1974. *Adsorption on solids*. London: Butterworth and Co.

Powers, M. C. 1967. "Fluid-release mechanisms in compacting marine mudrocks and their importance in oil exploration." *Am. Assoc. Pet. Geol. Bull.* 51 (7): 1240–1254. https://doi.org/10.1306/5D25C137-16C1-11D7-8645000102C1865D.

Revil, A., and N. Lu. 2013. "Unified water isotherms for clayey porous materials." *Water Resour. Res.* 49 (9): 5685–5699. https://doi.org/10.1002/wrcr.20426.

Robinson, J. D., and F. Vahedifard. 2016. "Weakening mechanisms imposed on California's levees under multiyear extreme drought." *Clim. Change* 137 (1): 1–14. https://doi.org/10.1007/s10584-016-1649-6.

Romero, E., A. Gens, and A. Lloret. 2001. "Temperature effects on the hydraulic behaviour of an unsaturated clay." *Geotech. Geol. Eng.* 19 (3/4): 311–332. https://doi.org/10.1023/A:1013133809333.

Romero, E., A. Gens, and A. Lloret. 2003. "Suction effects on a compacted clay under non-isothermal conditions." *Géotechnique* 53 (1): 65–81.

Roshani, P., and J. A. I. Sedano. 2016. "Incorporating temperature effects in soil water characteristics curves." *Indian Geotech. J.* 46 (3): 309–318. https://doi.org/10.1007/s40098-016-0201-y.

Salager, S., M. S. Ei Youssoufi, and C. Saix. 2007. "Influence of temperature on the water retention curve of soils. Modelling and experiments." In *Experimental unsaturated soil mechanics*, edited by T. Schanz, 251–258. Berlin: Springer.

Salager, S., M. S. El Youssoufi, and C. Saix. 2010. "Effect of temperature on water retention phenomena in deformable soils: Theoretical and experimental aspects." *Eur. J. Soil Sci.* 61 (1): 97–107. https://doi.org/10.1111/j.1365-2389.2009.01204.x.

Schneider, M., and K. U. Goss. 2011. "Temperature dependence of the water retention curve for dry soils." *Water Resour. Res.* 47 (3): W03506 https://doi.org/10.1029/2010WR009687.

Seki, K. 2007. "SWRC fit—A nonlinear fitting program with a water retention curve for soils having unimodal and bimodal pore structure." *Hydrol. Earth Syst. Sci. Discuss.* 4 (1): 407–437. https://doi.org/10.5194/hessd-4-407-2007.

Stormont, J. C., and C. E. Anderson. 1999. "Capillary barrier effect from underlying coarser soil layer." *J. Geotech. Geoenviron. Eng.* 125 (8): 641–648. https://doi.org/10.1061/(ASCE)1090-0241(1999)125:8(641).

Tang, A. M., and Y. J. Cui. 2005. "Controlling suction by the vapour equilibrium technique at different temperatures and its application in determining the water retention properties of MX80 clay." *Can. Geotech. J.* 42 (1): 287–296. https://doi.org/10.1139/t04-082.

Tuller, M., and D. Or. 2005a. "Water retention and soil water characteristics curve." In *Encyclopedia of soils in the environment*, edited by D. Hillel, 278–289. Amsterdam, Netherlands: Elsevier.

Tuller, M., and D. Or. 2005b. "Water films and scaling of soil characteristic curves at low water contents." *Water Resour. Res.* 41 (9): W09403 https://doi.org/10.1029/2005WR004142.

Tuller, M., D. Or, and L. Dudley. 1999. "Adsorption and capillary condensation in porous media: Liquid retention and interfacial configurations in angular pores." *Water Resour. Res.* 35 (7): 1949–1964. https://doi.org/10.1029/1999WR900098.

Uchaipichat, A., and N. Khalili. 2009. "Experimental investigation of thermo-hydro-mechanical behaviour of an unsaturated silt." *Geotechnique* 59 (4): 339–353. https://doi.org/10.1680/geot.2009.59.4.339.

Vahedifard, F., A. AghaKouchak, E. Ragno, S. Shahrokhabadi, and I. Mallakpour. 2017. "Lessons from the Oroville Dam." *Science* 355 (6330): 1139–1140. https://doi.org/10.1126/science.aan0171.

Vahedifard, F., A. AghaKouchak, and J. D. Robinson. 2015. "Drought threatens California's levees." *Science* 349 (6250): 799. https://doi.org/10.1126/science.349.6250.799-a.

Vahedifard, F., J. D. Robinson, and A. AghaKouchak. 2016. "Can protracted drought undermine the structural integrity of California's earthen levees?" *J. Geotech. Geoenviron. Eng.* 142 (6): 02516001. https://doi.org/10.1061/(ASCE)GT.1943-5606.0001465.

van Genuchten, M. T. 1980. "A closed-form equation for predicting the hydraulic conductivity of unsaturated soils." *Soil Sci. Soc. Am. J.* 44 (5): 892–898. https://doi.org/10.2136/sssaj1980.03615995004400050002x.

Villar, M. V., and R. Gomez-Espina. 2007. "Retention curves of two bentonites at high temperature." In Vol. 112 of *Experimental unsaturated soil mechanics: Springer Proceedings in Physics*, edited by T. Schanz, 267–274. Berlin: Springer.

Villar, M. V., and A. Lloret. 2004. "Influence of temperature on the hydro-mechanical behaviour of a compacted bentonite." *Appl. Clay Sci.* 26 (1–4): 337–350. https://doi.org/10.1016/j.clay.2003.12.026.

Villar, M. V., P. L. Martin, and A. Lloret. 2005. "Determination of water retention curves of two bentonites at high temperature." In *Advanced experimental unsaturated soil mechanics. Experus*, edited by A. Tarantino, E. Romero, and Y. J. Cui, 77–82. London: A.A. Balkema Publishers.

Wan, M., W. M. Ye, Y. G. Chen, Y. J. Cui, and J. Wang. 2015. "Influence of temperature on the water retention properties of compacted GMZ01 bentonite." *Environ. Earth Sci.* 73 (8): 4053–4061. https://doi.org/10.1007/s12665-014-3690-y.

Watson, K. M. 1943. "Thermodynamics of the liquid state." *Ind. Eng. Chem.* 35 (4): 398–406. https://doi.org/10.1021/ie50400a004.

Wersin, P., L. H. Johnson, and I. G. McKinley. 2007. "Performance of the bentonite barrier at temperature beyond 100°C. A critical review." *Phys. Chem. Earth.* 32 (8–14): 780–788. https://doi.org/10.1016/j.pce.2006.02.051.

Ye, W. M., Y. W. Zhang, B. Chen, Y. G. Chen, and Y. J. Cui. 2012. "Investigation on compressibility of highly compacted GMZ01 bentonite with suction and temperature control." *Nucl. Eng. Des.* 252 (Nov): 11–18. https://doi.org/10.1016/j.nucengdes.2012.06.037.

Young, T. 1805. "An essay on the cohesion of fluids." *Philos. Trans. R. Soc. London* 95: 65–87. https://doi.org/10.1098/rstl.1805.0005.

Zheng, L., J. Rutqvist, J. T. Birkholzer, and H. H. Liu. 2015. "On the impact of temperatures up to 200°C in clay repositories with bentonite engineer barrier systems: A study with coupled thermal, hydrological, chemical, and mechanical modelling." *Eng. Geol.* 197 (Oct): 278–295. https://doi.org/10.1016/j.enggeo.2015.08.026.

Zhou, A.-N., D. Sheng, and J. Li. 2014. "Modelling water retention and volume change behaviours of unsaturated soils in non-isothermal conditions." *Comput. Geotech.* 55 (Jan): 1–13. https://doi.org/10.1016/j.compgeo.2013.07.011.